EFFECTS OF DIFFERENT ENTRY FLOW PROFILES ON THERMAL STRIPING IN MIXING T-JUNCTION

L. Lampunio*, Y. Duan, M.D. Eaton

Nuclear Engineering Group, Department of Mechanical Engineering, City and Guilds Building (CAGB), Imperial College London, Exhibition Road, South Kensington Campus, United Kingdom (UK), SW7 2BX.

ABSTRACT

This paper investigates the effects of different inlet velocity profiles on thermal mixing within a T-junction. The flow domain is modelled using the Improved Delayed Detached Eddy Simulation (IDDES-SST) turbulence model implemented within the commercial CFD solver STAR-CCM+ 2020.1.1. The OECD/NEA-Vattenfall experimental benchmark database is used to validate the CFD model. The influence of different inlet flow profiles on CFD simulations is then assessed. Different combinations of inlet flow profiles at different developing stages are considered within the CFD simulations, for a total of eight cases. These inlet flow profiles are generated with RANS k-ω-SST models for both inlet pipes and supplied to the T-junction inlets for the IDDES simulations. The generated profiles of velocity, turbulent kinetic energy, specific dissipation rate, and temperature profiles are then supplied as inlet BCs of the T-junction computational model. It is found that the distribution of temperature on the pipe wall is highly affected by the inlet flow profiles of the branch pipe. A uniform entry profile at the branch inlet causes higher values of mean temperature at the top of the pipe and higher values of temperature variance at the sides of the pipe. A fully developed entry profile used at the main inlet produces instead higher values of mean and variance of temperature compared to cases that use uniform profiles at the main inlet. The velocity distribution exhibits also noticeable differences among the cases. Specifically, cases that use non-uniform entry profiles at the branch inlet present a stronger velocity gradient and a bigger recirculation area downstream the T-junction.

1. INTRODUCTION

Thermal striping is defined as the fluctuating temperature field imposed on the surface of a structure such as a pipe. This is usually caused by the incomplete turbulent mixing of fluids at different temperatures. Thermal striping within the piping systems of nuclear power plants (NPPs), where fluids of different temperature meet such as T-junctions, can cause high-cycle thermo-mechanical stresses and potentially induce fatigue cracks (Chapuliot et al. [1]). The leakage incident of Civaux 1 Pressurized Water Reactor (PWR) is an example of pipe-crack initiated by thermal fatigue associated with temperature fluctuations in a mixing T-junction of the residual heat removal system [1].

Several CFD studies have been performed to study the thermal mixing within T-junctions (Smith et al. [2], Braillard et al. [3]). It is concluded that LES provides the most accurate results for such problems. However, LES simulations are computationally demanding, as they require a fine mesh close to the wall for a wall resolved simulation (Jayarajua et al. [4]). Alternatively, hybrid LES-RANS models, such as the DES model, can produce accurate results comparable to LES (Kang et al. [5]). An accurate choice of boundary conditions (BCs) is also fundamental for an accurate prediction of temperature fluctuations in the fluid domain, as they could introduce model errors and additional uncertainty (Schmidt [6]).

This paper investigates the effect of entry flow profiles on the thermal mixing within T-junctions. Several combinations of different velocity profiles are used. The computational model replicates the geometry of the Vattenfall T-junction experimental test rig and it is validated against the OECD/NEA-Vattenfall T-junction Benchmark experimental data [2].

*Corresponding Author: l.lampunio18@imperial.ac.uk

2. METHODOLOGY

The commercial CFD software STAR-CCM+ version 2020.1.1 is used to model and simulate the Vattenfall T-junction experiment used in the OECD/NEA-Vattenfall benchmark (STARCCM+ 2020.1.1 Manual [7])[2]. The schematics of the experimental test rig and of the computational domain are presented in Figure 1. The experimental test rig consists of a horizontal (main) pipe with diameter of 140 mm where water at 19°C flows with constant flow rate of 9 l/s, and vertical (branch) pipe with diameter of 100 mm which carries water at 36°C at 6 l/s. The length of the pipes upstream the T-junction is more then 80 diameters for the main pipe and around 20 diameters for the branch pipe. This means that fully developed conditions are reached only in the main pipe at the T-junction inlet. Further information can be found here [2].

The flow domain in the T-junction and outlet pipe is modelled with the IDDES-SST turbulence model (Shur et al. [8]), the MUSCL 3rd order central difference spatial discretization scheme is utilised, and the prescribed time step size is 5×10^{-4} s, which gives a CFL number lower than 0.5. The turbulent heat flux is modelled with the simple gradient diffusion hypothesis. An additional RANS k-ω-SST model (Menter [9]) is used to model the flow in the main and branch inlet pipes and to calculate the BCs for the IDDES-SST model. Turbulent quantities, such as turbulent kinetic energy and specific dissipation rate, velocity and temperature values, obtained from these RANS simulations, are supplied at the inlets of the T-junction computational model.

Three different mesh resolutions are used to perform a mesh sensitivity study and validate the computational model. To validate the computational model, the experimental conditions are first reproduced. Therefore, the BCs prescribed at the T-junction inlets are extracted from the RANS simulations at 80 and 20 diameters of the main and branch inlet pipe, respectively. This process is applied to the three different mesh resolutions used in the mesh sensitivity analysis. The model is extensively validated, and the results of the mesh sensitivity study can be found here (Lampunio et al. [10]). The finest mesh is chosen for these simulations.

The BCs used in this study are also extracted from the RANS simulations and extracted at different x-position along the branch and main pipes at 20, 40 and 60 diameters downstream of the pipes' inlets. Uniform BCs are also considered for both pipes and refer to the bulk flow properties. Figure 2 presents the entry velocity profiles BCs used in our study and extracted from the RANS simulations, compared to the BCs used in the benchmark exercise. For the sake of completeness, the BCs extracted for the mesh sensitivity study are also presented for the finest mesh resolution.

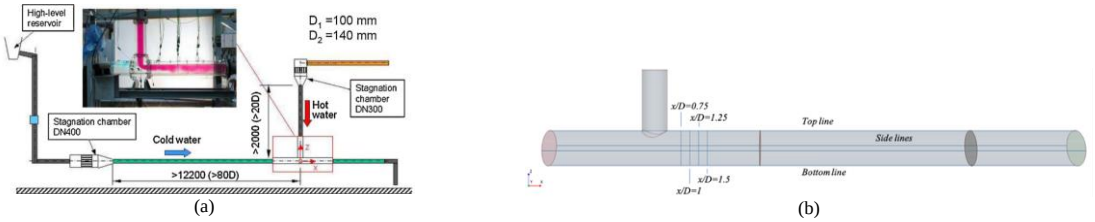

Figure 1 Schematic of the test rig (a) and computational domain (b) with locations of display of quantities of interest.

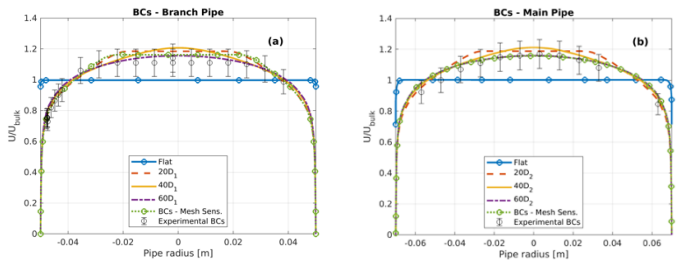

Figure 2 Velocity entry profiles used in this study for the T-junction branch inlet (a) and T-junction main inlet (b).

3. RESULTS

In total, eight cases are developed, and each case is identified by two indices which are indicative of the BCs prescribed at the T-junction inlets. The first index refers to the main inlet BCs and the second one to the branch inlet. '0' refers to uniform profiles, whereas '60' to fully developed conditions.

The IDDES-SST model applies the RANS model near the wall (RANS region) and uses the LES model away from the wall (LES region). The two models are combined based on the IDDES length scale, l_{IDDES}, defined as [8]:

$$l_{IDDES} = \tilde{f}_d(1 + f_e)l_{RANS} + (1 - \tilde{f}_d)l_{LES}$$

Where the functions $\tilde{f}_d$ and f_e are, respectively, the blending and elevating function, and l_{RANS} and l_{LES} are the RANS and LES length scale. The blending function $\tilde{f}_d$ gives an estimate of the RANS/LES regions across the computational domain and it varies from 0 in RANS mode, to 1 in LES mode [7]. The values of $\tilde{f}_d$ on the XZ symmetry plane and at different cross sections along the x-axis are presented for the cases considered in this study in Figure 3. It can be seen that the region covered by the RANS model at the top part of the pipe downstream the T-junction is quite narrow in all cases. This is the area where the jet flow from the branch pipe detaches, and a strong recirculation bubble is formed. The regions of RANS model in the lower part of the pipe are instead wider for all cases since the jet flow does not reach the opposite wall.

The biggest discrepancies in the values of $\tilde{f}_d$ are witnessed in the jet entrance region, close to the upstream corner of the T-junction. Cases with uniform velocity profiles applied at the branch inlet, 0-0 and *60-0*, show LES regions upstream the T-junction and along the upstream vertical branch wall. This might indicate a possible detachment of the main flow from the upstream corner in the upper part of the pipe with formation of recirculation zones and flow entrainment along the vertical wall (see Figure 3 0-0,60-0). The LES regions at these locations seem to decrease as the velocity profiles applied at the branch inlet reach a more developed stage (cases *0-20*, *0-40*, *0-60*, *60-20*, *60-40*, and *60-60*). Cases with uniform velocity profiles at the main inlet, cases *0-0*, *0-20*, *0-40*, and *0-60*, exhibit LES regions very close to the wall at the cross section passing though the T-junction central axis, where the main and jet flows meet. This might indicate the formation of secondary flow and small vortices that could influence the mixing in the upper part of the pipe and cause a lower temperature distribution in this area (see Figure 5(b)(e)(c)(f) and Figure 7). It must be stressed that these plots represent just a qualitative estimation of the RANS/LES regions and further investigations are needed to confirm and quantitatively describe the different underlying flow structures among these cases.

The streamwise velocity, U/U_{bulk}, at different locations downstream the T-junction is illustrated in Figure 4. From this, it can be seen that the recirculation area downstream the T-junction is much smaller and less intense in the cases with uniform BCs at the branch inlet. The recirculation area for cases where non-uniform BCs are used at the branch inlet occupies instead almost half of the pipe section and the velocity in this area is maximum close to the top wall, resulting in a stronger velocity gradient (Figure 4(c)(d)). The fluid flowing below the jet is also more accelerated due to a more intense Venturi effect, see Georgiou et al. [11].

The fluid mean temperature, $T^* = (\overline{T} - T_{cold})/\Delta T$ and the root mean square (rms) of its variance $T^*_{rms} = \sqrt{\overline{(T')^2}}/\Delta T$ are shown in Figure 5 and Figure 6 for the top, bottom, and side lines, at 1 mm distance from the wall. The top view of T^* and $T^*_{var} = \overline{(T')^2}/\Delta T^2$ on the pipe wall are illustrated in Figure 7 and Figure 8, respectively. The value of T^* in the upper half of the pipe is higher when the uniform flow profile is applied at the branch inlet, i.e. for cases *0-0* and *0-60*, see Figure 5(b)(c)(e)(f), and Figure 7. The highest T^* at the wall is observed for the combination *0-60* (Figure 7). The other six cases present lower values of T^* and a more uniform distribution at the top wall (Figure 5 and Figure

7). Among these cases the ones with fully developed profiles at the main inlet, *60-20*, *60-40*, and *60-60*, produce slightly higher values of T^* at the top and sides, compared to cases *0-20*, *0-40*, and *0-60* (Figure 5(e)(f), and Figure 7). Values of T^*_{rms} and T^*_{var} are shown in Figure 6 and Figure 8. The combination 0-0 results in the lowest value of temperature fluctuations at the top and bottom of the pipe and the highest value at the sides, see Figure 6 (a)(b)(d)(e), and Figure 8. Cases *0-20*, *0-40*, *0-60*, *60-20*, *60-40*, and *60-60* show that the region of maximum variance moves toward the top of the pipe (Figure 8). It is interesting to note that, amongst these cases, the variance at the sides is higher when fully developed conditions are used at the main pipe, i.e. *60-20*, *60-40*, and *60-60*.

Figure 5 and Figure 6 also present the results from the benchmark exercise. It can be seen that, for cases with uniform velocity profiles at the branch pipe, cases *0-0* and *60-0*, both T^* and T^*_{rms} substantially deviate from the experimental data. These two cases overestimate T^* at the top and sides of the pipe. T^*_{rms} is much higher close to the T-junction for the sides of the pipe but is very underpredicted at the top. Cases with *0-20*, *0-40*, and *0-60* tend to underestimate, close to the T-junction, T^* at the top and both T^* and T^*_{rms} for the sides. An overall better agreement is found for cases with fully developed profiles at the main pipe and non-uniform profiles at the branch pipe, with the closest agreement achieved with the combination *60-20* which is very similar to the benchmark experimental conditions.

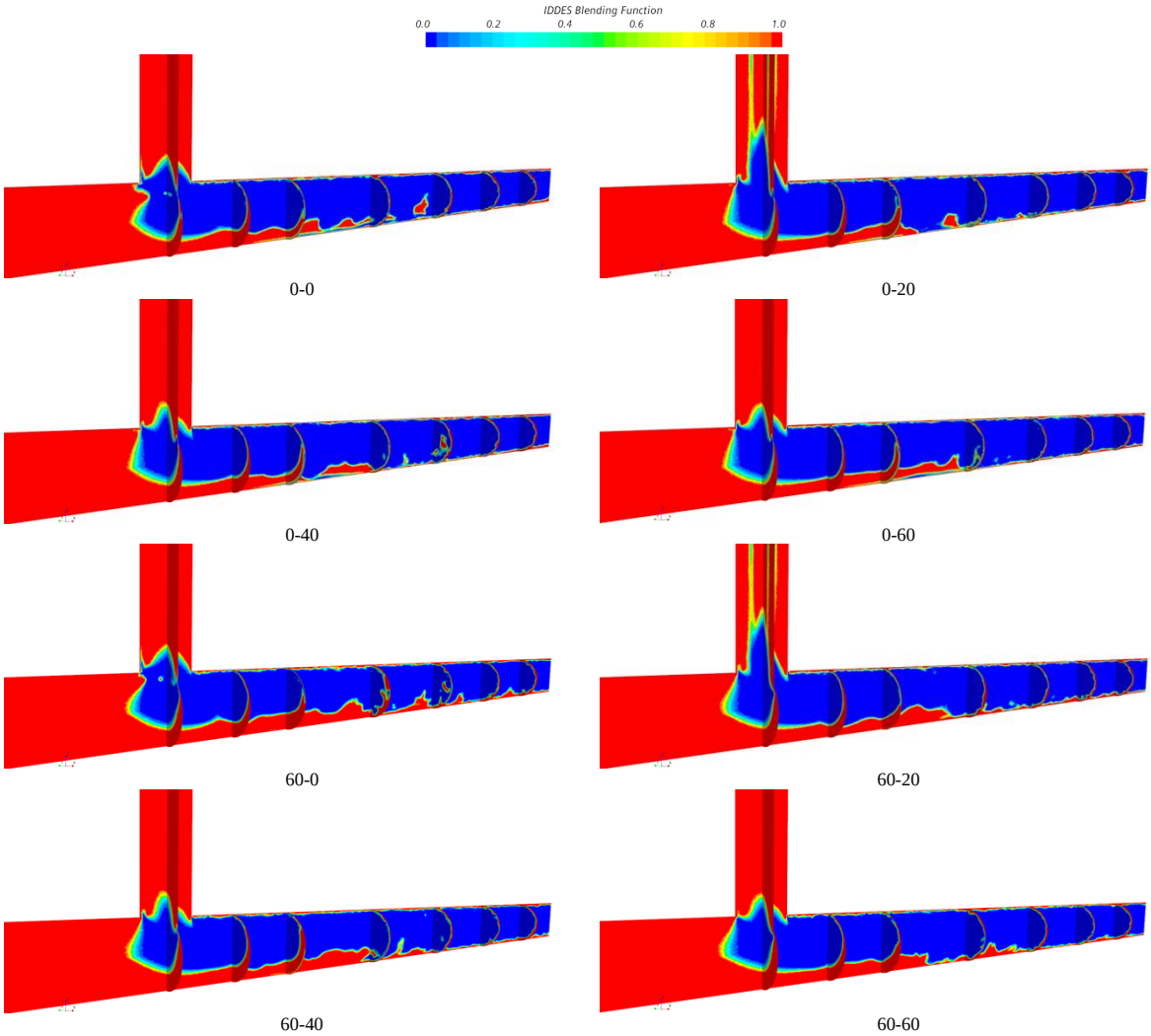

Figure 3 Contours of $\tilde{f}_d$ on XZ symmetry plane and cross sections located at $x/D_2 = 0, 1, 2, 4, 6, 8, 10$. The IDDES model switches to LES where $\tilde{f}_d = 0$ (blue regions), whereas RANS is used where $\tilde{f}_d = 1$ (red regions).

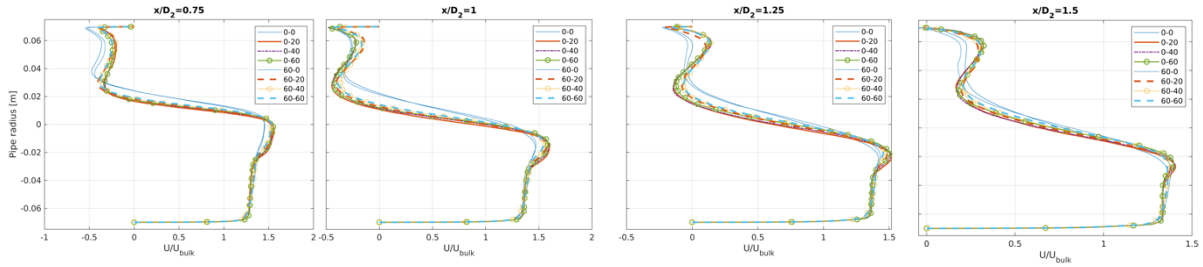

(a) (b) (c) (d)

Figure 4 Profiles of U/U_{bulk} at different cross-section along the x-axis.

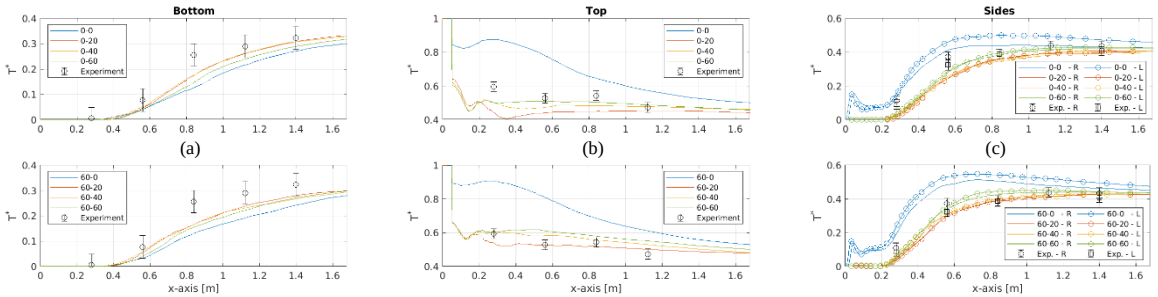

(a) (b) (c) (d) (e) (f)

Figure 5 Profiles of T^* at bottom (a), (d), top (b), (e), and sides (c), (f) pipe.

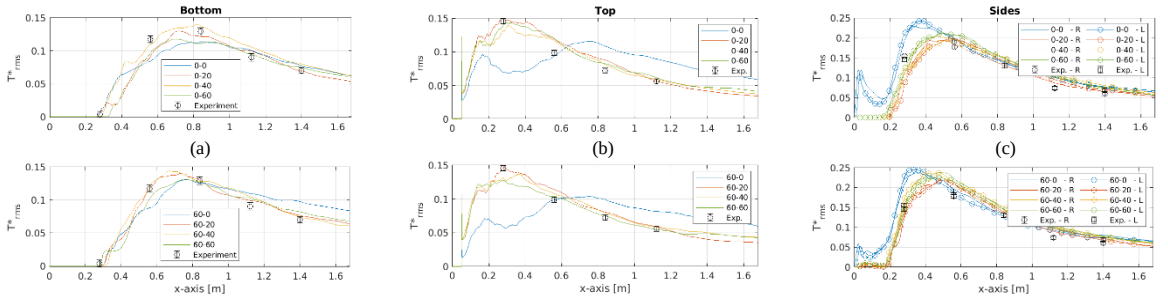

(a) (b) (c) (d) (e) (f)

Figure 6 Profiles of T^*_{rms} at bottom (a), (d), top (b), (e), and sides (c), (f) pipe.

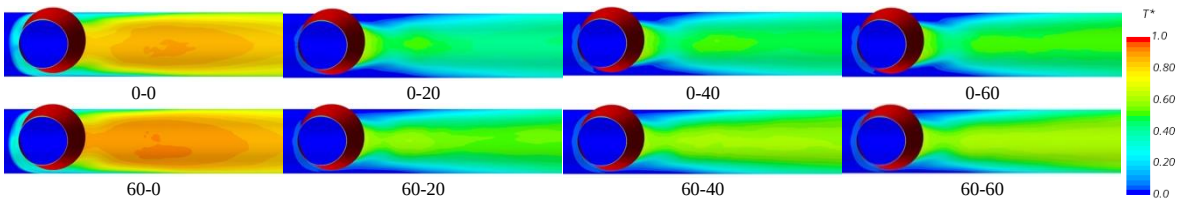

Figure 7 Top view of T^* at the pipe wall.

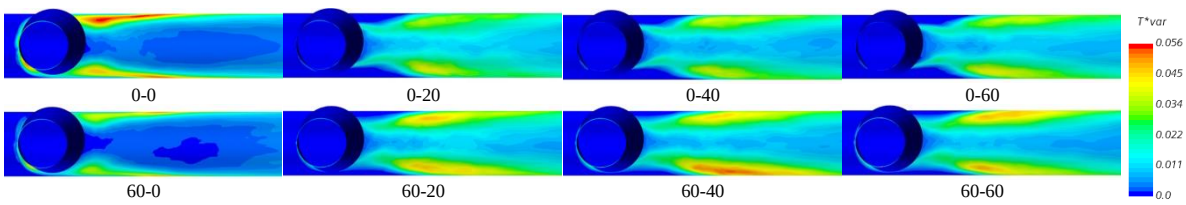

Figure 8 Top view of T^*_{var} at the pipe wall.

4. CONCLUSIONS

CFD simulations of thermal striping in mixing T-junction have been performed with the IDDES model. The computational model is based on the Vattenfall T-junction experimental test rig and is validated against the OECD/NEA-Vattenfall benchmark data. Different BCs at the T-junction inlets are prescribed and their effects on the wall temperature and on the mean velocity field are assessed. It is found that the mixing of fluids at the top of the pipe, as well as the location of the largest variance in the quantities of interest are mainly affected by the BCs of the branch inlet. The mixing is weaker when using uniform BCs are prescribed at the branch inlet and this results in the highest temperature at the top wall and the largest variance in the temperature at the sides, which could lead higher thermal stresses within the pipe wall. The BCs prescribed at the main inlet influence instead the magnitude of the mean temperature and its variance on the wall surface. With fully developed BCs at the main inlet, higher values are observed overall.

REFERENCES

[1] S. Chapuliot, C. Gourdin, T. Payen, J.P. Magnaud & A. Monavon, Hydro-thermal-mechanical analysis of thermal fatigue in a mixing tee. *Nucl. Eng. Des.*, **235** (2005) 575-596

[2] B.L. Smith, J.H. Mahaffy, K. Angele & J. Westin, Report of the OECD/NEA-Vattenfall T-Junction Benchmark exercise. Nuclear Energy Agency, Report No. NEA/CSNI/R(2011)5 1–92 (2011).

[3] O. Braillard, R. Howard, K. Angele, A. Shams & N. Edh, Thermal mixing in a T-junction: Novel CFD-grade measurements of the fluctuating temperature in the solid wall. *Nucl. Eng. Des.*, **230** (2018) 377-390

[4] S.T. Jayarajua, E.M.J. Komena & E. Baglietto, Suitability of wall-functions in Large Eddy Simulation for thermal fatigue in a T-junction. *Nucl. Eng. Des.*, **240** (2010) 2544–2554

[5] D. G. Kang, H. Na & C. Y. Lee, Detached eddy simulation of turbulent and thermal mixing in a T-junction. *Annals of Nuclear Energy*, **124** (2019)

[6] J. Schmidt, *Process and Plant Safety Applying Computational Fluid Dynamics*

[7] Siemens Industries Digital Software. Simcenter STAR-CCM+, version 2020.1.1, Siemens 2020

[8] M.L. Shur, P.R. Spalart, M.K Strelets & A.K. Travin, A hybrid RANS-LES approach with delayed-DES and wall-modelled LES capabilities. *Int. J. of Heat & Fluid Flow*, **29** (2008) 1638–49

[9] F.R. Menter, Two-equation eddy-viscosity turbulence models for engineering applications. *American Institute of Aeronautics and Astronautics Journal*, **32** (1994).

[10] L. Lampunio, Y. Duan, R. Issa & M. Eaton, Thermal stripping analysis in T-junctions with different entry flow profiles. Advances in Thermal Hydraulics 2020 (ATH 2020) Conference proceeding.

[11] M. Georgiou & M. V. Papalexandris, Turbulent mixing in T-junctions: The role of the temperature as an active scalar. *Int. J. Heat Mass Transfer*, **115** (2017) 2017 793–809